Open access • Posted Content • DOI:10.1101/402495

Role of STING complex in differential retrograde signaling in cybrids with K versus H haplogroup mtDNA — Source link

Kevin Schneider, Marilyn Chwa, Atilano, Sonali Nashine ...+7 more authors

Institutions: University of California, Irvine, Tulane University

Published on: 28 Aug 2018 - bioRxiv (Cold Spring Harbor Laboratory)

Topics: Haplogroup, Human mitochondrial DNA haplogroup and STING complex

Related papers:

- Mitochondrial DNA variants can mediate methylation status of inflammation, angiogenesis and signaling genes
- The impact of mitochondrial and nuclear DNA variants on late-onset Alzheimer's disease risk.
- Mitochondrial DNA Copy Number (mtDNA-CN) Can Influence Mortality and Cardiovascular Disease via Methylation of Nuclear DNA CpGs
- Blood-derived mitochondrial DNA copy number is associated with gene expression across multiple tissues and is predictive for incident neurodegenerative disease
- Mitochondrial transcription factor A variants and the risk of Parkinson's disease.

Share this paper:

View more about this paper here: https://typeset.io/papers/role-of-sting-complex-in-differential-retrograde-signaling-30x6nhcbax

bioRxiv preprint doi: https://doi.org/10.1101/402495; this version posted August 28, 2018. The copyright holder for this preprint (which was not certified by peer review) is the author/funder, who has granted bioRxiv a license to display the preprint in perpetuity. It is made available under aCC-BY 4.0 International license.

1 7-03-18
2

3 Role of STING complex in differential retrograde signaling
4 in cybrids with K versus H haplogroup mtDNA

5
6
7
8 Kevin Schneider[1], Marilyn Chwa[1], Shari R. Atilano[1], Sonali Nashine[1], Nitin Udar[1], David S. Boyer[2], S. Michal
9 Jazwinski[3], Michael V. Miceli[3], Anthony B. Nesburn[1,4], Baruch D. Kuppermann[1], M. Cristina Kenney[1, 5]
10
11
12 *[1]Department of Ophthalmology, Gavin Herbert Eye Institute, University of California Irvine, Irvine, CA 92697*
13 *[2]Retina-Vitreous Associates Medical Group; Beverly Hills, CA 90211*
14 *[3]Tulane Center for Aging and Department of Medicine, Tulane University, New Orleans, LA 70112*
15 *[4]Cedars-Sinai Medical Center, Los Angeles, CA 90048*
16 *[5]Department of Pathology and Laboratory Medicine, University of California Irvine, Irvine, CA 92697*
17
18
19
20
21 **Conflicts of Interest/Disclosures: None.**
22
23
24
25 **Address correspondence to:**
26 M. Cristina Kenney, M.D., Ph.D.
27 Professor, Ophthalmology
28 Gavin Herbert Eye Institute, Ophthalmology Research Laboratory
29 University of California Irvine
30 Hewitt Hall, Room 2028
31 843 Health Science Road
32 Irvine, CA 92697
33 Telephone: (949) 824-7603
34 Fax: (949) 824-9626
35 Email mkenney@uci.edu
36

bioRxiv preprint doi: https://doi.org/10.1101/402495; this version posted August 28, 2018. The copyright holder for this preprint (which was not certified by peer review) is the author/funder, who has granted bioRxiv a license to display the preprint in perpetuity. It is made available under aCC-BY 4.0 International license.

38
39
40 **ABSTRACT**
41

42 Mitochondrial (mt) DNA haplogroups, defined by specific single nucleotide polymorphism (SNPs) patterns,
43 represent populations of diverse geographic origins and may play a role in disparate disease susceptibilities found in
44 different ethnic/racial populations. The most common European haplogroup is H, while the K haplogroup is highly
45 associated with Ashkenazi Jewish populations. Studies using transmitochondrial cybrids (cell lines with identical nuclei
46 but mitochondria from either H or K haplogroup subjects) demonstrated significant molecular and biological differences
47 but mechanisms for these disparities are unclear. In this study, we hypothesized that there is differential retrograde
48 signaling occurring between the Stimulator of Interferon Genes (STING) pathway and H versus K mtDNA haplogroups.
49 Results showed that K cybrids exhibit increased levels of cytoplasmic mtDNA fragments. After STING Knock-Down, H
50 cybrids had lower expression levels for *EGFR, BRCA1, DNMT3A*, *DNMT3B, HDAC1,* and *IFNα* genes, but upregulated
51 *DNMT3A* compared to control H cybrids. The STING-KD K cybrids showed downregulation of *EGFR, DNMT3A,*
52 *HDAC1, HCAD9, CFH*, and *CHI,* along with upregulation of *DNMT1* and *IL-6* compared to control K cybrids. Since all
53 cybrids have identical nuclei, the STING DNA sensor system interacts differently with K haplogroup mtDNA compared
54 to H mtDNA for genes related to cancer (*EGFR, BRCA1*), methylation (*DNMT1, DNMT3A, DNMT3B*), acetylation
55 (*HDAC1, HDCA9*), complement (*CFH, CHI*) and inflammation (*IFNα, IL-6*). In summary, in non-pathologic conditions,
56 (a) STING is an important retrograde signaling mechanism(s) and (b) cybrids possessing Ashkenazi Jewish mtDNA (K
57 haplogroup) interact with the STING complex differently compared to H cybrids which affects various disease-related
58 pathways.

bioRxiv preprint doi: https://doi.org/10.1101/402495; this version posted August 28, 2018. The copyright holder for this preprint (which was not certified by peer review) is the author/funder, who has granted bioRxiv a license to display the preprint in perpetuity. It is made available under aCC-BY 4.0 International license.

60 **INTRODUCTION**

61 Mitochondria (mt) possess unique circular DNA that is maternally inherited. The mtDNA encodes for 37 genes,
62 including 13 protein subunits essential for oxidative phosphorylation (OXPHOS), 2 ribosomal RNAs and 22 transfer
63 RNAs. (1-3) The non-coding region of 1121 nucleotides, known as the MT-Dloop, is critical for mtDNA replication and
64 transcription. Recent studies report that small biologically active peptides called Humanin and MOTsC that encoded from
65 the *16s* and *12s* rRNA regions of the mtDNA, respectively, are likely involved in various pathological processes. (4, 5)
66 All cells have both nuclear and mitochondrial genomes contributing to disease processes. The transmitochondrial cybrids,
67 which are cell lines with identical nuclei but the mtDNA from different subjects, have been used to identify the effects of
68 an individual's mtDNA upon cellular homeostasis.(6-9) Previous studies using transmitochondrial cybrids (cell lines with
69 identical nuclei but mtDNA from either H or K haplogroup subjects) have shown that the K cybrids have (a) significantly
70 lower mtDNA copy numbers, (b) higher expression levels for MT-DNA encoded genes critical for oxidative
71 phosphorylation, (c) lower Spare Respiratory Capacity (SRC), (d) increased expression of inhibitors of the complement
72 pathway and important inflammasome-related genes; (e) significantly higher levels of *APOE* transcription that were
73 independent of methylation status; and (f) higher levels of resistance to amyloid-$\beta_{1\text{-}42}$ peptides (active form) than the H
74 haplogroup cybrids(10), but it has been unclear how the differential retrograde signaling occurs in H versus K cybrids.
75 Previously, we have used the human retinal pigment epithelial (RPE) cybrid model to show that cybrids with K
76 haplogroup mtDNA have (1) significantly increased expression of ApoE, a critical lipid transporter molecule associated
77 with human diseases; (2) higher degree of protection from cytotoxic effects of amyloid-$\beta_{1\text{-}42}$ (active form); (3) increased
78 expression of inhibitors of the alternative complement pathways and important inflammation-related genes; and (4)
79 elevated bioenergetic respiratory profiles compared to the H cybrids.(10) These findings suggest that an individual's K
80 haplogroup mtDNA contributes to lipid transport, cholesterol metabolism, complement activation and inflammation,
81 factors critical for AMD, Alzheimer's disease and other age-related diseases. However, the mechanisms of retrograde
82 signaling by different mtDNA variants (K versus H haplogroup) to the nucleus are not known at this time.

83 It is recognized that diverse racial/ethnic populations have different risks for specific diseases. For example,
84 African-Americans are susceptible to developing type 2 diabetes, obesity, prostate cancer and glaucoma. (11-14) and
85 European-Caucasians are more prone to developing age-related macular degeneration (AMD), skin cancers, carotid artery
86 disease and multiple sclerosis. (15, 16) The maternal origins of different human populations can be classified into
87 haplogroups based upon the patterns of accumulated single nucleotide polymorphisms (SNPs) within the mtDNA. Either

bioRxiv preprint doi: https://doi.org/10.1101/402495; this version posted August 28, 2018. The copyright holder for this preprint (which was not certified by peer review) is the author/funder, who has granted bioRxiv a license to display the preprint in perpetuity. It is made available under aCC-BY 4.0 International license.

88 increased risk or protection for human diseases, including Alzheimer's disease, AMD, cancers and diabetes, can be
89 associated with the mtDNA haplogroup profile of the subjects. (2, 17-28)

90 The H haplogroups are the most common European mtDNA haplogroup, while the L haplogroups, representing
91 individuals of maternal African-origin, are the oldest and most diversified haplogroup (www.MitoMap.com). The
92 A12308G SNP defines the UK cluster that contains both the U and K haplogroups. The K haplogroups (also known as
93 Uk) is further defined by the G9055A SNP, has a 1-6% worldwide distribution and represents approximately 10% of
94 ancestral Europeans. Approximately 32% of Ashkenazi Jewish population is highly associated with the K haplogroup and
95 can be classified into the K1a1b1a, K2a2a and K1a9 subsets. (15) The genetic profile of the Ashkenazi Jewish population
96 has become more homogeneous because of limited numbers of founders, intermarriage within the group and population
97 bottlenecks involving decreases in population sizes due to environmental and/or sociological events. (29)Behar, 2004
98 #7040} As a result, with respect to the genetic profiles, the Ashkenazi Jewish population is an excellent well-defined
99 group for studies correlating genetics associations with specific diseases including hypercholesteremia, hyperlipidemia,
100 cardiovascular disease, Gaucher disease type 1, Usher Type 3A, Tay-Sachs disease and *BRCA1/BRCA2* genes associated
101 with breast and ovarian cancers. (30-34)

102 The STING (Stimulator of Interferon Genes) pathway represents a DNA sensor pathway used by cells to detect
103 the presence of cytoplasmic DNA fragments, which then trigger activation of innate immune systems (Fig. 1). (35) The
104 vast majority of research about STING has investigated the effects of viral and bacterial infections releasing intracellular,
105 foreign DNA that activates the host defenses.(36, 37) STING can also be activated by "self-DNA" resulting in
106 autoimmune disease such as Systemic Lupus Erythematosus (SLE) and Aicardi-Goutie syndrome.(38) It was recently
107 shown that transfection of PCR-amplified mtDNA fragments into ARPE-19 cells induced inflammatory cytokines and the
108 effects were blocked following knock-down of STING.(39) Interestingly, these effects were dependent on the size of the
109 mtDNA fragments but not sequence or location. Previous studies have shown that different racial/ethnic mtDNA
110 haplogroups are associated with varying disease susceptibilities and innate immune responses.(7, 10, 16, 40) To our
111 knowledge, this is the first study to investigate whether the STING system is engaged in non-pathological signaling
112 between the mtDNA and nuclear genome and whether using the cybrid model, the different haplogroups (e.g., H versus
113 K) might elicit different responses in downstream genes from cells that have identical nuclei and culture conditions.

114

115

bioRxiv preprint doi: https://doi.org/10.1101/402495; this version posted August 28, 2018. The copyright holder for this preprint (which was not certified by peer review) is the author/funder, who has granted bioRxiv a license to display the preprint in perpetuity. It is made available under aCC-BY 4.0 International license.

116 **MATERIALS AND METHODS**

117 *Generating Cybrid Cell Lines and Culture Conditions:* Institutional review board approval was obtained from the
118 University of California, Irvine (#2003-3131). There was no significant difference between the ages of the H subjects (n
119 = 4, 42.5 ± 7.3 years) and K subjects (n = 5, 48.4 ± 3.6, p = 0.46) (Table 1).

120 Peripheral blood was collected in sodium citrate tubes and DNA isolated using the DNA extraction kit
121 (PUREGENE, Qiagen, Valencia, CA). Using a series of centrifugation steps, platelets were isolated, suspended in Tris
122 buffer saline (TBS) and then fused with ARPE-19 cells that were deficient in mtDNA (Rho*0*) as described previously (9).
123 Cybrids were cultured until confluent in DMEM-F12 containing 10% dialyzed fetal bovine serum, 100 unit/ml penicillin
124 and 100 µg/ml streptomycin, 2.5 µg /ml fungizone, 50 µg/ml gentamycin and 17.5 mM glucose. All experiments used
125 passage 5 cybrid cells.

126 *Protein extraction:* H and K cybrid cell lines were plated in six-well plates for 48 hours. Cells were lysed using
127 RIPA buffer (Cat. # 89900, Life Technologies), supernatants transferred to a new microfuge tube and concentrations of
128 proteins were measured using Bio-Rad Dc protein assay system (Bio-Rad Laboratories, Richmond, CA, USA) according
129 to the manufacturer's instructions.

130 *Immunoblotting:* Equal concentrations of total protein samples were loaded into the wells of 4–12% Bolt mini
131 gels (Life Technologies) followed by SDS-PAGE electrophoresis. The gels were then transferred onto PVDF membranes.
132 Following transfer, the membranes were blocked in 5% BSA/TBST for 1 hour, and incubated overnight at 4°C in primary
133 antibodies. Blots were then washed with three times in TBST (Tris Buffered Saline-Tween20) and incubated with the
134 respective secondary antibodies for 1 hour at room temperature. All primary and secondary antibodies were diluted in 5%
135 BSA/TBST or 5% Milk/TBST as per manufacturer's instructions. Following secondary antibody incubation, the blots
136 were washed three times in TBST. Protein bands were detected using Clarity Western ECL Blotting Substrate (Cat.
137 #1705060, Bio-Rad). β-actin antibody was used as a housekeeper protein control. Protein bands were visualized using
138 Versadoc imager (Bio-Rad), and quantified using ImageJ software (NIH Image).

139 *Statistical Analyses:* Data were subjected to statistical analysis by unpaired t-test, GraphPad Prism (Version 5.0,
140 La Jolla, CA). $P<0.05$ was considered statistically significant. Error bars in the graphs represent SEM (standard error
141 mean).

142 *Knock-down of STING:* For siRNA mediated knockdown of STING, cybrid ARPE cells were seeded in 6-well
143 plates at 7x10^5 cells/well. Thirty pmol final concentration of STING siRNA (#128591, ThermoFisher/Ambion,

bioRxiv preprint doi: https://doi.org/10.1101/402495; this version posted August 28, 2018. The copyright holder for this preprint (which was not certified by peer review) is the author/funder, who has granted bioRxiv a license to display the preprint in perpetuity. It is made available under aCC-BY 4.0 International license.

144 Waltham, MA) or Scramble siRNA were diluted in OPTI-MEM (ThermoFisher/Invitrogen) and incubated at room
145 temperature for 5 minutes. Transfection reagent Lipofectamine 2000 (Invitrogen) was then mixed separately with OPTI-
146 MEM as per manufacturer's protocol and incubated for 5 minutes at room temperature. The OPTI-MEM/siRNA and
147 OPTI-MEM/Lipofectamine tubes were then combined and incubation was carried out for 5 minutes at room temperature
148 to allow formation of siRNA-lipid complex. Final mixture was then applied to cybrid cells in culture and allowed to
149 incubate for 48 hours before RNA isolation.

150 *Isolation of RNA and Amplification of cDNA:* RNA was isolated from untreated and STING-KD cultures (H
151 cybrids, n=4; K cybrids, n=5) using the RNeasy Mini-Extraction kit (Qiagen) as described previously.(9) cDNA
152 generated from 2 μg of individual RNA samples with the QuantiTect Reverse Transcription Kit (Qiagen) was used for
153 qRT-PCR analyses.

154 *Quantitative Real-time PCR (qRT-PCR) Analyses:* Total RNA was isolated from individual pellets of cultured
155 haplogroup H cybrid cells (n=4 different individuals) and K cybrid cells (n=5 different individuals) as described above.
156 qRT-PCR was performed on individual samples using QuantiFast SYBR Green PCR Kits (Qiagen) on an Applied
157 Biosystems ViiA7 real time quantitative PCR detection system. Primers (QuantiTect Primer Assay, Qiagen or KicqStart
158 Primers, Sigma) used to analyze for 37 different genes in various pathway: Complement *(CFH, CD59, CD55/DAF, CFI*);
159 Methylation (*DNMT1, TRDMT1, DNMT3A, DNMT3B*); Acetylation (*HDAC1*, *HDAC2*, *HDAC3, HDAC4, HDAC6,*
160 *HDAC9, HDAC10, HDAC11, HAT1*); Inflammation (*IL-6*, *IL-33*, *IL1β*, *IL-18*, *IFNα*, *IFNβ*; Chemokines (*CCL2*, *CCL20*);
161 Cancer (*EGFR*, *BRCA1*, *ERBB2*, *ALK*, *PD1*); and STING pathway genes (*CGAS, TBK1, IRF3, IkBa, NFKB2, TRAF2,*
162 *TNFRSF19*). Primers were standardized with the *HPRT1* or *HMBS* housekeeping genes. All analyses were performed in
163 triplicate.

164 *Identification of Cytoplasmic DNA:* Cells from cybrid cultures were collected (H cybrids, n = 4 and K cybrids, n
165 = 5) and divided into two equal aliquots (1×10^6 cells per aliquot). One set of aliquots was used for whole cell DNA
166 extraction utilizing DNeasy Blood and Tissue kits (Qiagen) and these extracts served as normalization controls for the
167 mtDNA copy numbers (see above). The second set of aliquots was resuspended in 500 μl buffer containing 50 mM
168 HEPES (pH 7.4), 150 mM NaCl, and 25 μg/ml digitonin (MilliporeSigma, St. Louis, MO). The digitonin homogenates
169 were incubated for ten minutes at room temperature on an end-over-end rocker to allow for selective plasma membrane
170 permeabilization. Samples were then centrifuged at 1000*g* for three minutes to pellet intact cells. The supernatants were
171 transferred to new tubes and spun at 17,000*g* for 10 minutes at room temperature to pellet any debris. This final spin

bioRxiv preprint doi: https://doi.org/10.1101/402495; this version posted August 28, 2018. The copyright holder for this preprint (which was not certified by peer review) is the author/funder, who has granted bioRxiv a license to display the preprint in perpetuity. It is made available under aCC-BY 4.0 International license.

172 yielded the cytosolic fraction. Cytoplasmic DNA was isolated and purified from this cytosolic fraction using the
173 QIAQuick Nucleotide Removal Columns (Qiagen).
174
175 **RESULTS**
176
177 **K haplogroup cybrids exhibit increased mitochondrial DNA fragments in the cytoplasm:**
178 Total cytoplasmic DNA was extracted from H and K cybrids (n=3) and analyzed for expression of both
179 mitochondrial DNA markers (MT-ND2) and nuclear DNA markers (Actin). Cytoplasmic DNA content was then
180 normalized to the total DNA. Mitochondrial DNA target expression was normalized to nuclear target expression, and
181 overall cytoplasmic content normalized to total DNA levels (Fig. 2A). The K cybrids contained 4.3 fold higher levels of
182 mitochondrial DNA in the cytoplasmic fraction compared to H cybrids. (p=0.049)
183
184 **Mitochondrial haplogroup does not affect STING gene expression:**
185 The STING complex is the intracellular sensor system for DNA fragments. Altered expression of downstream
186 genes after STING knock-down is indicative that the DNA fragments are playing a role in the transcription for those
187 genes. Gene expression levels for STING at baseline were similar between H and K cybrids (Fig. 2B). The H (n = 5) and
188 K (n = 5) cybrids underwent STING knockdown (KD) by transfecting the cells with 30pmol siRNA or Silencer negative
189 control. After 48 hours, RNA was isolated and the expression levels of the STING gene were measured by qRT-PCR.
190 STING expression was significantly decreased in both the H and K cybrid cells. (11.48%, p=0.0028 in H cybrids and
191 9.5%, p<0.0001 in K cybrids; Fig. 2B). Gene expression was then analyzed for pathways related to cancer, epigenetics,
192 complement and inflammation.
193
194 **Haplogroup K cybrids exhibit decreased expression of key DNA methylation genes:**
195 The K cybrids had lower levels of expression for DNMT1 (77.7% ± 4.3, p = 0.0057), *DNMT3B* (54.6% ± 3.4, p
196 0.0042) and *TRDMT1* (73.1% ± 4.2, p = 0.035), and DNMT3a (60.0% ± 2.7, p=0.0179) compared to the H cybrids. The
197 levels for *MAT2B* were similar in the H and K cybrids (Fig. 3a). The expression levels for genes related to acetylation
198 (*HDAC1, HDAC2*, *HDAC3*, *HDAC4*, *HDCA6*, *HDAC9*, and *HDCA11*) were similar in the H and K cybrids at baseline
199 (Fig. 3b).

bioRxiv preprint doi: https://doi.org/10.1101/402495; this version posted August 28, 2018. The copyright holder for this preprint (which was not certified by peer review) is the author/funder, who has granted bioRxiv a license to display the preprint in perpetuity. It is made available under aCC-BY 4.0 International license.

200 **Knockdown of STING alters expression of epigenetic genes dependent on mitochondrial haplogroup:**

201 After STING-KD, *DNMT3A* gene expression dropped in both H and K cybrids (H: 68.2% ± 5.6, p=0.05; K:
202 43.9% ± 3.6, p=0.03) compared to the Control cybrids (Fig. 3a). *DNMT1* expression levels were increased significantly in
203 both cybrids (H: 175.3% ± 7.4, p<0.0001; K: 163.4% ± 16.1, p=0.0009) compared to the Control H and K cybrids. For
204 *DNMT3B*, the expression levels were lower in the STING-KD H cybrids (70.9% ± 3.9, p = 0.05) but not in the STING-
205 KD K cybrids (p = 0.17). *TRDMT1 (DNMT2)* is a highly conserved methyl transferase that showed no change in
206 expression after STING-KD in the H (p = 0.76) or K (p = 0.41) cybrids. The *HDAC1* expression decreased in both H and
207 K cybrids after STING-KD (H: 69.2% ± 5.7, p=0.016; K: 80.8% ± 5.6, p=0.0009) versus Control cybrids (Fig.4b). The
208 STING-KD K cybrid had lower levels of HDAC9 (70.9% ± 7.9, p = 0.02) while the expression levels in the STING-KD H
209 cybrids were decreased compared to Control cybrids but was not significant (p = 0.18). STING-KD did not affect
210 expression levels of *HDAC2*, *HDAC3*, *HDC4*, *HDAC6*, *HDAC9*, *HDAC10, HDAC11* and *HAT1* in the H or K cybrids
211 (Fig. 3b).

212

213 **Haplogroup K cybrids differentially express markers of inflammation and RPE differentiation:**

214 The untreated K cybrids had lower levels of *IFNα* (54.2% ± 9.6, p = 0.006) and *CCL2* (24.6% ± 5.4, p = 0.0005)
215 but higher levels of *IFNβ* (163.7% ± 12.2, p = 0.029) and *IL33* (185.3% ± 19.3, p = 0.04) compared to untreated H
216 cybrids. The levels for *CCL20* (p = 0.08), *IL6* (p = 0.11), *IL1β* (p = 0.52) and *NLRP3* (p = 0.31) were similar in the
217 untreated H and K cybrids.

218

219 **Knockdown of STING alters expression of inflammatory genes dependent on mitochondrial haplogroup:**

220 In the STING-KD K cybrids there was a decrease in *CFI* (72.6% ± 7.2, p=0.0045) and *CFH* (48.2% ± 3.1%,
221 p=0.036; Fig. 4b). There was increased transcription levels in *IL6* (300.3.1% ± 44.6%, p=0.02) compared to K Control
222 cybrids (160% ± 19.7%). The STING-KD H cybrids showed lower expression of *IFNα* (80.9% ± 5.3%, p = 0.04)
223 compared to Control K cybrids. After STING-KD, there were no changes in expression levels for *CD55*, *CD59*, *CCL2*,
224 *CCL20*, *IFNβ*, and *IL33* in either the H or K cybrids (Fig. 4a).

225

226

227

bioRxiv preprint doi: https://doi.org/10.1101/402495; this version posted August 28, 2018. The copyright holder for this preprint (which was not certified by peer review) is the author/funder, who has granted bioRxiv a license to display the preprint in perpetuity. It is made available under aCC-BY 4.0 International license.

228 **K haplogroup cybrids exhibit decreased expression of key cancer target genes:**

229 The cancer genes investigated in this study are known targets for drugs that are currently being used clinically to
230 treat cancer patients (Table 2). The K cybrids had significantly lower expression levels of four cancer related genes
231 (*BRCA1*, 51.6% ± 9.9%, p = 0.007; *EGFR*, 73.9% ± 6.9%, p = 0.05; *ALK*, 22.6% ± 5.9%, p = 0.003 and *PD1*, 40.5% ±
232 12.6%, p = 0.03) compare to H cybrids. The transcription levels for *ERBB2* (p = 0.3) were similar in H and K cybrids
233 (Fig. 5a).

234

235 **Knockdown of STING influences BRCA1 and EGFR gene expression dependent on haplogroup:**

236 After STING-KD, the H cybrids showed lower *BRCA1* expression levels (34.7% ± 11.1%, p = 0.02) compared to
237 H Control cybrids, while the K cybrid showed no significant decrease (p = 0.41). Conversely, the *EGFR* levels were
238 lower in the STING-KD K cybrids (29.1% ± 10.1%, p = 0.02) and also in the STING-KD H cybrids (28.1% ± 11.8%, p =
239 0.05) compared to the untreated cybrids. The levels for *ALK*, *PD1*, and *ERBB2* were similar in the STING-KD versus
240 Control H and K cybrids (Fig. 5a).

241

242 **K haplogroup cybrids differentially express genes involved in the STING DNA sensing pathway:**

243 A variety of genes involved in the STING signaling pathway were analyzed and we discovered that K cybrids had
244 higher expression of *IkBa* (194.0% ± 30.2%, p = 0.05) and *NFKB2* (145.1% ± 11.9%, p = 0.026) as well as lower
245 expression of *TNFRSF19* (27.5% ± 7.9%, p = 0.0073) and *IRF3* (67.9% ± 5.1%, p = 0.009) at baseline compared to H
246 cybrids (Fig. 5b). At baseline there were no differences in expression of *CGAS*, *TBK1* or *TRAF2* between H and K
247 cybrids.

248

249 **Knockdown of STING increases expression of *IRF3* in K haplogroup cybrids***:*

250 After STING-KD, the only gene affected was *IRF3*, which was increased in the K cybrids compared to the lower
251 baseline value (107.2% ± 8.7%, p = 0.0081). Interestingly, this increase returned *IRF3* gene expression to comparable
252 levels of the untreated H cybrids. The levels of *CGAS, TBK1, TRAF2, IkBa, NFKB2*, and *TNFRSF19* were similar in
253 STING-KD H and K cybrids (Fig. 5b).

254

255

bioRxiv preprint doi: https://doi.org/10.1101/402495; this version posted August 28, 2018. The copyright holder for this preprint (which was not certified by peer review) is the author/funder, who has granted bioRxiv a license to display the preprint in perpetuity. It is made available under aCC-BY 4.0 International license.

256 **K haplogroup cybrids exhibit decreased phosphor-IRF protein levels:**

257 In order to confirm expression levels of key STING pathway genes and identify any alterations in STING
258 signaling at baseline between the H and K cybrids, protein expression was measured via western blot. Phosphorylated and
259 non-phosphorylated antibodies were used because many key STING pathway proteins function through phosphorylation.
260 K cybrids demonstrated increased levels of IRF3 protein level (596% ± 58.3, p = 0.0015) and a decrease in the level of
261 phospo-IRF3 (59.3% ± 10.8, p = 0.021) when compared to baseline H cybrids (Figs. 6a, 6b). No difference was seen in
262 expression of NFKB or phosphor-NKFB (Figs. 6c- 6e).

263

264 **DISCUSSION**

265 The present study was designed to determine if the STING (*TMEM-173*) pathway was involved in the signaling
266 from the mitochondria to the nuclear genome in cybrids containing mitochondria from healthy subjects with either
267 common European H haplogroup mtDNA or the Ashkenazi Jewish associated K haplogroup mtDNA. Studies have shown
268 altered expression levels of genes associated with epigenetic pathways in K versus H cybrids and that inhibition of
269 methylation with 5-aza-2'-deoxycytidine (5-aza-dC) altered the expression of NFκβ2, an important transcription factor
270 activation of inflammation and immunity. (10)

271 The present study was designed to determine if activation of STING via DNA fragments played a role in the
272 modulation of five methylation-related genes and eight acetylation-related genes. After STING-KD, both H and K cybrids
273 showed increased expression of *DNMT1* and lower expression of *DNMT3A.* However, only the STING-KD H cybrids
274 showed reduced *DNMT3B* expression levels while the STING-KD K cybrids were similar to control K cybrids. These
275 findings indicate that the transcription of methylation pathway genes (*DNMT1, DNMT3A* and *DNMT3B*) can be regulated
276 through STING, an intracellular DNA sensor system, and more importantly, the transcription levels are differentially
277 expressed if the cells possess K haplogroup mtDNA compared to H haplogroup mtDNA. This potentially could lead to
278 alterations in methylation patterns and variable modulation of downstream genes, depending if the subject has European
279 mtDNA haplogroup versus Ashkenazi Jewish mtDNA profiles.

280 Of the eight acetylation genes investigated, only the *HDAC1* expression levels were reduced in both the H and K
281 cybrids after STING-KD. This finding suggests that in non-pathological, unstressed cells there are some levels of STING
282 activation via DNA fragmentation that upregulate HDAC1, a Class I histone deacetylase important for proliferation
283 differentiation and apoptosis. This is the first description of a relationship between STING activation and modulation of

bioRxiv preprint doi: https://doi.org/10.1101/402495; this version posted August 28, 2018. The copyright holder for this preprint (which was not certified by peer review) is the author/funder, who has granted bioRxiv a license to display the preprint in perpetuity. It is made available under aCC-BY 4.0 International license.

284 HDACs. Interestingly, in the STING-KD K cybrids the *HDAC9* transcription was significantly lower (p = 0.02) while the
285 STING-KD H cybrids showed a trend for lower *HDAC9* levels but it did not reach significant (p = 0.18) due to larger
286 variations within the H cybrids. *HDAC9,* which is important for mitochondrial functions, has highest expression in brain
287 (41) and has not previously been reported to be expressed in human RPE cells. *HDAC9* inhibits *Mef2* (myocyte enhancer
288 factor2), which is important to oxidative phosphorylation in conventional T cells and T-regulatory (Treg) cells. (42)
289 *HDAC9* also plays a role in Treg suppressive functions and inhibits transcription of *PGC1α* and *Sirt3*, both important for
290 mitochondrial replication and ROS metabolism. These data suggest that via the STING pathway, the mtDNA can mediate
291 the *HDAC9* expression levels, thereby influencing the mitochondria metabolism and possibly immune functions.
292 However, additional studies are needed to more fully understand this relationship. The other six acetylation genes showed
293 similar levels before and after STING knock-down.

294 The mechanism by which the STING complex affects the epigenetics is unknown. However, it has been shown
295 that nuclear envelope transmembrane protein 23 (NET23)/STING can promote chromatin condensation and induce
296 epigenetic changes, which is important because of its role in signaling for innate and apoptosis.(6) Green and coworkers
297 reported that in response to viral-like double stranded RNA, the Pacific oyster (*Crassostrea gigas*) showed a upregulation
298 of virus recognition receptors, signaling and effector genes, but the DNA methylation genes and STING remained
299 unchanged, consistent with a poorly developed immune priming response. (43) This suggests that in mammalian cells,
300 the activation of STING along with altered expression of specific methylation and acetylation genes may be important for
301 immune recognition but the individual's responses may be unique depending upon the ethnic/racial origin and underlying
302 mtDNA profile.

303 It is recognized that pathological conditions (e.g., viral and bacterial infections) are often associated with DNA
304 fragmentation and STING activation that modulates the immune responses. However, our findings suggest that STING
305 activation may also be important for retrograde (mitochondria to nucleus) signaling under non-pathogenic conditions. In
306 this study, the H and K haplogroup cybrid cell lines have identical nuclei and are cultured under non-stressed conditions.
307 One can speculate that the fragmentation of the H mtDNA (European) versus the K mtDNA (Ashkenazi Jewish) might
308 yield different size or variants of fragments that then activate the STING pathway differently, thereby leading to
309 differences in the downstream regulation of the epigenetic genes. Our data shows that K haplogroup cybrids have
310 increased levels of mtDNA in the cytoplasm of these cells. Due to the influence of this mtDNA load on the STING
311 pathway, this could cause differences in methylation status, which might play a role in personalized responses to drugs

bioRxiv preprint doi: https://doi.org/10.1101/402495; this version posted August 28, 2018. The copyright holder for this preprint (which was not certified by peer review) is the author/funder, who has granted bioRxiv a license to display the preprint in perpetuity. It is made available under aCC-BY 4.0 International license.

312 and diseases that are often seen in the Ashkenazi Jewish populations. Using the cybrid model, higher levels of total global
313 methylation have also been reported in cell lines with the European J haplogroup (44, 45), Ashkenazi Jewish K
314 haplogroup (10), and also in cybrids with the African-origin L haplogroups (*unpublished data*) compared to those with the
315 H haplogroup mtDNA. In turn, methylation patterns can influence the homeostasis of mitochondria, affecting apoptosis
316 (46-48), and can be associated with disease susceptibilities and prognoses for cancers and age-related diseases. (49)

317 The field of therapies for cancer patient has been revolutionized by development of drugs targeting specific
318 molecules key for progression and prognosis of the cancer. However, in spite of the use of these 'targeting-drugs' there
319 are still many cancer victims that fail treatment and it is often not understood why they fail. In this study we analyzed the
320 H versus K cybrids for the expression levels for 4 genes targeted by drugs; (a) Cetuximab, Erlotinib, Gefitinib and
321 Lapatinib are inhibitors for *EGFR* production; (b) Crizotinibi, Ceritinib and Alectinib are inhibitors for *ALK*; (c)
322 Pembrolizumab and Nivolumab are inhibitors of *PD1;* and (d) Pertuzumab and Trastuzumab targets the *ERBB2* (*HER2*)
323 gene. We found that the untreated control H cybrids (European) had significantly higher expression of four of the genes
324 (*EGFR*, p = 0.05; *BRCA1*, p = 0.007; *ALK*, p = 0.003; and *PD1*, p = 0.034) compared to the untreated K cybrids
325 (Ashkenazi Jewish). After STING-KD for both H and K cybrids, the expression levels of *EGFR* were decreased (28.1%,
326 p = 0.05 and 29.1%, p = 0.02, respectively) indicating that the *EGFR* is partially modulated via this DNA sensing system.
327 Our findings suggest that the DNA fragments and STING pathway may be novel and previously unrecognized pathways
328 to target for *EGFR* modulation in cancer patients.

329 If the cybrid findings are representative of what might be occurring in cancer patients, then there would be
330 differential expression levels for these important genes, with European patients (H haplogroup) having higher
331 transcription levels than Ashkenazi Jewish (K haplogroup) patients. Due to lower expression levels, K haplogroup
332 patients might not respond equally to the inhibitor drugs for those gene products. This phenomenon may account for
333 some of the differential responses found in clinical drug trials and also in prognosis outcomes for the cancer patients. It
334 suggests that perhaps evaluation of the individual mtDNA profile may be of benefit to designing their treatment protocols.
335 However, additional investigations are required fully understand the relationship between a person's mtDNA haplogroup
336 and their response to anti-cancer medications. In any case, this is the first report showing that the mtDNA variants can
337 influence gene expression levels of these critical cancer-related genes.

338 The reported prevalence of BRCA1/2 mutation is has been reported to be higher in the Ashkenazi Jewish
339 population (1 in 40) compared to other populations (1 in 400-800 persons). The expression levels of *BRCA1*, a gene

bioRxiv preprint doi: https://doi.org/10.1101/402495; this version posted August 28, 2018. The copyright holder for this preprint (which was not certified by peer review) is the author/funder, who has granted bioRxiv a license to display the preprint in perpetuity. It is made available under aCC-BY 4.0 International license.

340 highly associated with approximately 40% of inherited breast cancers and 80% of inherited breast and ovarian cancers,
341 were also measured in K versus H cybrids. With respect to the *BRCA1* gene, the H cybrids had higher levels to begin with
342 but showed a 34.7% decline after STING-KD ($p = 0.02$). In contrast, the K cybrids, with lower initial levels, were not
343 affected by STING-KD. As *BRCA1* encodes for a tumor suppressor, individuals of the Ashkenazi Jewish population with
344 the K haplogroup, may be expressing lower levels of this tumor inhibitor and therefore have less protection against cancer
345 development.

346 Many of the studies related to the STING complexes are within the confines of viral infections. For example, it
347 was reported that as herpes viruses induce mtDNA stress, the anti-viral signaling increases, leading to heightened
348 responses of type I interferon. (36) While it is recognized that mitochondria are key participants in innate immunity
349 required for robust anti-viral responses, our findings suggest that the STING sensor system is also a pathway of
350 communication in healthy cells. This is not surprising as the symbiotic relationship between mitochondria and eukaryotic
351 cells occurred over time and ancient signaling system would likely be maintained for cellular homeostasis (Fig. 6b).

352 K cybrids exhibit differential expression of several key genes associated with the STING pathway and its
353 inflammatory response. Our data shows that K cybrids demonstrate increased gene expression of NFκβ2, an important
354 gene associated with the inflammatory pathway of STING. This is consistent with the increased - mtDNA detected in the
355 cytoplasm of K cybrids. However, western blot detected no difference of either NFκβ2 or phosphor-NFκβ2 levels between
356 H and K cybrids (*data not shown*). Interestingly, there was decreased gene expression of *IRF3*, and decreased protein
357 levels for phopho-*IRF3* in K cybrids. IRF3 and NκβB are critical to the STING pathway, which induces antiviral and pro-
358 inflammatory cytokines, including type I interferons (IFN-α and IFN-β). Additionally, untreated K cybrids exhibited
359 increased expression of *IkBa*, an inhibitor of NFκβ, but showed no difference in the expression of other key STING
360 pathway related genes, such as *CGAS, TBK1* and *TRAF2*. The majority of data surrounding the STING complex has
361 focused on its response to viral and bacterial infections, demonstrating that exogenous mtDNA can induce cellular
362 inflammatory responses. However, our cybrid system is unique in that the mtDNA present in the cytoplasm is
363 endogenous, rather than exogenous. Additionally, since the cells are under no external stress, the increased cytoplasmic
364 content of mtDNA found in the K cybrids could be viewed as their normal state or non-pathogenic retrograde signaling.

365 The data from this study demonstrates that mitochondrial DNA haplogroup can exert a powerful effect on nuclear
366 gene expression (Fig. 7a). One potential method by which mitochondrial DNA is able to elicit these changes is through
367 the use of mitochondrial DNA fragments as signaling molecules (Fig. 7b). Most interestingly, there are subsets of genes

bioRxiv preprint doi: https://doi.org/10.1101/402495; this version posted August 28, 2018. The copyright holder for this preprint (which was not certified by peer review) is the author/funder, who has granted bioRxiv a license to display the preprint in perpetuity. It is made available under aCC-BY 4.0 International license.

368 that are differentially regulated by STING, dependent on mitochondrial haplogroup. This suggests that response to
369 mtDNA fragments can be influenced by the mtDNA background. Additionally, this data demonstrates an association
370 between mitochondrial haplogroup and mtDNA fragments levels. These fragments do not always illicit a pathogenic
371 response, as would be expected. Finally, our data has identified novel pathways influenced by the expression of STING,
372 suggesting that sensing of mtDNA fragments can have far reaching implications for signaling outside of inflammation.
373

374
375
376
377
378
379
380
381
382
383
384
385
386
387
388
389
390
391
392
393
394
395

bioRxiv preprint doi: https://doi.org/10.1101/402495; this version posted August 28, 2018. The copyright holder for this preprint (which was not certified by peer review) is the author/funder, who has granted bioRxiv a license to display the preprint in perpetuity. It is made available under aCC-BY 4.0 International license.

396 **FUNDING**

397 This work was supported by the Discovery Eye Foundation, Polly and Michael Smith, Iris and the B. Gerald
398 Cantor Foundation, Beckman Initiative for Macular Research, Max Factor Family Foundation, and the National Institute
399 on Aging [AG006168 to SMJ]. We acknowledge the support of the Institute for Clinical and Translational Science
400 (ICTS) at UCI. The authors acknowledge departmental support from an RPB unrestricted grant.

401

---

bioRxiv preprint doi: https://doi.org/10.1101/402495; this version posted August 28, 2018. The copyright holder for this preprint (which was not certified by peer review) is the author/funder, who has granted bioRxiv a license to display the preprint in perpetuity. It is made available under aCC-BY 4.0 International license.

403
ACKNOWLEDGEMENTS

404 We wish to thank the subjects who participated in this study.

405
406
407
408
409
410
411
412
413
414
415
416
417
418
419
420
421
422
423
424
425
426
427
428
429
430
431
432
433
434
435
436
437
438
439

bioRxiv preprint doi: https://doi.org/10.1101/402495; this version posted August 28, 2018. The copyright holder for this preprint (which was not certified by peer review) is the author/funder, who has granted bioRxiv a license to display the preprint in perpetuity. It is made available under aCC-BY 4.0 International license.

440 **FIGURE and TABLE LEGENDS**

441

442 **Figure 1.** The STING (Stimulator of Interferon Genes) pathway.

443 **Figure 2.** a) K haplogroup cybrids exhibit increased mitochondrial DNA fragments in the cytoplasm. b) Gene expression
444 levels for STING at baseline were similar between H and K cybrids.

445 **Figure 3.** Haplogroup K cybrids exhibit decreased expression of key DNA methylation genes. a) The levels for *MAT2B*
446 were similar in the H and K cybrids. b) The expression levels for genes related to acetylation (*HDAC1, HDAC2*, *HDAC3*,
447 *HDAC4*, *HDCA6*, *HDAC9*, and *HDCA11*) were similar in the H and K cybrids at baseline.

448 **Figure 4**. a) After STING-KD, there were no changes in expression levels for *CD55, CD59, CCL2, CCL20, IFNβ*, and
449 IL33 in either the H or K cybrids. b) In the STING-KD K cybrids there was a decrease in *CFI* (72.6% ± 7.2, p=0.0045)
450 and *CFH* (48.2% ± 3.1%, p=0.036).

451 **Figure 5.** Gene expression levels in H and K cybrids. a) Knockdown of STING influences *BRCA1* and *EGFR* gene
452 expression dependent on haplogroup and b) Knockdown of STING increases expression of *IRF3* in K haplogroup cybrids.

453 **Figure 6.** a, b) Phosphorylated and non-phosphorylated antibodies were used because many key STING pathway proteins
454 function through phosphorylation. K cybrids demonstrated increased levels of IRF3 protein level (596% ± 58.3, p =
455 0.0015) and a decrease in the level of phospo-IRF3 (59.3% ± 10.8, p = 0.021) when compared to baseline H cybrids. c)
456 No difference was seen in expression of NFKB or phosphor-NKFB.

457 **Figure 7.** a) Nuclear gene expression influenced by haplogroup, STING and differentially by both Haplogroup and
458 STING. b) One potential method by which mitochondrial DNA is able to elicit these changes is through the use of
459 mitochondrial DNA fragments as signaling molecules..

460 **Table 1.** Subject information including cybrid numbers, gender, age, and haplogroups.

461 **Table 2.** Description of Genes Targeted by Anti-cancer Drugs. The cancer genes investigated in this study are known
462 targets for drugs that are currently being used clinically to treat cancer patients.

---

bioRxiv preprint doi: https://doi.org/10.1101/402495; this version posted August 28, 2018. The copyright holder for this preprint (which was not certified by peer review) is the author/funder, who has granted bioRxiv a license to display the preprint in perpetuity. It is made available under aCC-BY 4.0 International license.

464 **CONFLICT OF INTEREST STATEMENT**

465 The authors have no conflict of interest to report.

466

467

468

bioRxiv preprint doi: https://doi.org/10.1101/402495; this version posted August 28, 2018. The copyright holder for this preprint (which was not certified by peer review) is the author/funder, who has granted bioRxiv a license to display the preprint in perpetuity. It is made available under aCC-BY 4.0 International license.

REFERENCES

1 Wallace, D.C. (1992) Diseases of the mitochondrial DNA. *Annu Rev Biochem*, 61, 1175-1212.

2 Wallace, D.C. (1994) Mitochondrial DNA mutations in diseases of energy metabolism. *J Bioenerg Biomembr*, 26, 241-250.

3 McFarland, R. and Turnbull, D.M. (2009) Batteries not included: diagnosis and management of mitochondrial disease. *J Intern Med*, 265, 210-228.

4 Yen, K., Lee, C., Mehta, H. and Cohen, P. (2013) The emerging role of the mitochondrial-derived peptide humanin in stress resistance. *Journal of molecular endocrinology*, 50, R11-19.

5 Lee, C., Yen, K. and Cohen, P. (2013) Humanin: a harbinger of mitochondrial-derived peptides? *Trends in endocrinology and metabolism: TEM*, 24, 222-228.

6 Malik, D., Hsu, T., Falatoonzadeh, P., Caceres-del-Carpio, J., Tarek, M., Chwa, M., Atilano, S.R., Ramirez, C., Nesburn, A.B., Boyer, D.S. *et al.* (2014) Human retinal transmitochondrial cybrids with J or H mtDNA haplogroups respond differently to ultraviolet radiation: implications for retinal diseases. *PLoS ONE*, 9, e99003.

7 Kenney, M.C., Chwa, M., Atilano, S.R., Falatoonzadeh, P., Ramirez, C., Malik, D., Tarek, M., Caceres-del-Carpio, J., Nesburn, A.B., Boyer, D.S. *et al.* (2014) Inherited mitochondrial DNA variants can affect complement, inflammation and apoptosis pathways: insights into mitochondrial-nuclear interactions. *Hum Mol Genet*, 23, 3537-3551.

8 Kenney, M.C., Chwa, M., Atilano, S.R., Falatoonzadeh, P., Ramirez, C., Malik, D., Tarek, M., Del Carpio, J.C., Nesburn, A.B., Boyer, D.S. *et al.* (2014) Molecular and bioenergetic differences between cells with African versus European inherited mitochondrial DNA haplogroups: implications for population susceptibility to diseases. *Biochim Biophys Acta*, 1842, 208-219.

9 Kenney, M.C., Chwa, M., Atilano, S.R., Pavlis, J.M., Falatoonzadeh, P., Ramirez, C., Malik, D., Hsu, T., Woo, G., Soe, K. *et al.* (2013) Mitochondrial DNA variants mediate energy production and expression levels for CFH, C3 and EFEMP1 genes: implications for age-related macular degeneration. *PLoS ONE*, 8, e54339.

10 Thaker, K., Chwa, M., Atilano, S.R., Coskun, P., Caceres-Del-Carpio, J., Udar, N., Boyer, D.S., Jazwinski, S.M., Miceli, M.V., Nesburn, A.B. *et al.* (2016) Increased expression of ApoE and protection from amyloid-beta toxicity in transmitochondrial cybrids with haplogroup K mtDNA. *Neurobiol Dis*, 93, 64-77.

11 Hatzfeld, J.J., LaVeist, T.A. and Gaston-Johansson, F.G. (2012) Racial/ethnic disparities in the prevalence of selected chronic diseases among US Air Force members, 2008. *Preventing chronic disease*, 9, E112.

12 Mensah, G.A., Mokdad, A.H., Ford, E.S., Greenlund, K.J. and Croft, J.B. (2005) State of disparities in cardiovascular health in the United States. *Circulation*, 111, 1233-1241.

13 Kurian, A.K. and Cardarelli, K.M. (2007) Racial and ethnic differences in cardiovascular disease risk factors: a systematic review. *Ethnicity & disease*, 17, 143-152.

14 Siegfried, C.J., Shui, Y.B., Holekamp, N.M., Bai, F. and Beebe, D.C. (2011) Racial differences in ocular oxidative metabolism: implications for ocular disease. *Arch Ophthalmol*, 129, 849-854.

15 Behar, D.M., Hammer, M.F., Garrigan, D., Villems, R., Bonne-Tamir, B., Richards, M., Gurwitz, D., Rosengarten, D., Kaplan, M., Della Pergola, S. *et al.* (2004) MtDNA evidence for a genetic bottleneck in the early history of the Ashkenazi Jewish population. *Eur J Hum Genet*, 12, 355-364.

16 Hendrickson, S.L., Jabs, D.A., Van Natta, M., Lewis, R.A., Wallace, D.C. and O'Brien, S.J. (2010) Mitochondrial haplogroups are associated with risk of neuroretinal disorder in HIV-positive patients. *J Acquir Immune Defic Syndr*, 53, 451-455.

17 Czarnecka, A.M. and Bartnik, E. (2011) The role of the mitochondrial genome in ageing and carcinogenesis. *Journal of aging research*, 2011, 136435.

bioRxiv preprint doi: https://doi.org/10.1101/402495; this version posted August 28, 2018. The copyright holder for this preprint (which was not certified by peer review) is the author/funder, who has granted bioRxiv a license to display the preprint in perpetuity. It is made available under aCC-BY 4.0 International license.

18 Strauss, K.A., DuBiner, L., Simon, M., Zaragoza, M., Sengupta, P.P., Li, P., Narula, N., Dreike, S., Platt, J., Procaccio, V. *et al.* (2013) Severity of cardiomyopathy associated with adenine nucleotide translocator-1 deficiency correlates with mtDNA haplogroup. *Proc Natl Acad Sci U S A*, 110, 3453-3458.

19 De Luca, A., Nasi, M., Di Giambenedetto, S., Cozzi-Lepri, A., Pinti, M., Marzocchetti, A., Mussini, C., Fabbiani, M., Bracciale, L., Cauda, R. *et al.* (2012) Mitochondrial DNA haplogroups and incidence of lipodystrophy in HIV-infected patients on long-term antiretroviral therapy. *J Acquir Immune Defic Syndr*, 59, 113-120.

20 Fernandez-Caggiano, M., Barallobre-Barreiro, J., Rego-Perez, I., Crespo-Leiro, M.G., Paniagua, M.J., Grille, Z., Blanco, F.J. and Domenech, N. (2013) Mitochondrial DNA haplogroup H as a risk factor for idiopathic dilated cardiomyopathy in Spanish population. *Mitochondrion*, 13, 263-268.

21 Canter, J.A., Kallianpur, A.R. and Fowke, J.H. (2006) Re: North American white mitochondrial haplogroups in prostate and renal cancer. *The Journal of urology*, 176, 2308-2309; author reply 2309.

22 Fernandez-Caggiano, M., Barallobre-Barreiro, J., Rego-Perez, I., Crespo-Leiro, M.G., Paniagua, M.J., Grille, Z., Blanco, F.J. and Domenech, N. (2012) Mitochondrial haplogroups H and J: risk and protective factors for ischemic cardiomyopathy. *PLoS ONE*, 7, e44128.

23 Bi, R., Zhang, W., Yu, D., Li, X., Wang, H.Z., Hu, Q.X., Zhang, C., Lu, W., Ni, J., Fang, Y. *et al.* (2015) Mitochondrial DNA haplogroup B5 confers genetic susceptibility to Alzheimer's disease in Han Chinese. *Neurobiol Aging*, 36, 1604 e1607-1616.

24 Ridge, P.G., Maxwell, T.J., Corcoran, C.D., Norton, M.C., Tschanz, J.T., O'Brien, E., Kerber, R.A., Cawthon, R.M., Munger, R.G. and Kauwe, J.S. (2012) Mitochondrial genomic analysis of late onset Alzheimer's disease reveals protective haplogroups H6A1A/H6A1B: the Cache County Study on Memory in Aging. *PLoS ONE*, 7, e45134.

25 Jones, M.M., Manwaring, N., Wang, J.J., Rochtchina, E., Mitchell, P. and Sue, C.M. (2007) Mitochondrial DNA haplogroups and age-related maculopathy. *Arch Ophthalmol*, 125, 1235-1240.

26 Udar, N., Atilano, S.R., Memarzadeh, M., Boyer, D.S., Chwa, M., Lu, S., Maguen, B., Langberg, J., Coskun, P., Wallace, D.C. *et al.* (2009) Mitochondrial DNA haplogroups associated with age-related macular degeneration. *Invest Ophthalmol Vis Sci*, 50, 2966-2974.

27 SanGiovanni, J.P., Arking, D.E., Iyengar, S.K., Elashoff, M., Clemons, T.E., Reed, G.F., Henning, A.K., Sivakumaran, T.A., Xu, X., DeWan, A. *et al.* (2009) Mitochondrial DNA variants of respiratory complex I that uniquely characterize haplogroup T2 are associated with increased risk of age-related macular degeneration. *PLoS ONE*, 4, e5508.

28 Kenney, M.C., Ferrington, D.A., Udar, N. (2013) *Mitochondrial Genetics of Retinal Diseases*. Elsevier.

29 Atzmon, G., Rincon, M., Rabizadeh, P. and Barzilai, N. (2005) Biological evidence for inheritance of exceptional longevity. *Mech Ageing Dev*, 126, 341-345.

30 Berchuck, A., Carney, M., Lancaster, J.M., Marks, J. and Futreal, A.P. (1998) Familial breast-ovarian cancer syndromes: BRCA1 and BRCA2. *Clinical obstetrics and gynecology*, 41, 157-166.

31 Guha, S., Rosenfeld, J.A., Malhotra, A.K., Lee, A.T., Gregersen, P.K., Kane, J.M., Pe'er, I., Darvasi, A. and Lencz, T. (2012) Implications for health and disease in the genetic signature of the Ashkenazi Jewish population. *Genome biology*, 13, R2.

32 Jenkins, T., Nicholls, E., Gordon, E., Mendelsohn, D., Seftel, H.C. and Andrew, M.J. (1980) Familial hypercholesterolaemia--a common genetic disorder in the Afrikaans population. *S Afr Med J*, 57, 943-947.

33 Lancaster, J.M., Carney, M.E. and Futreal, P.A. (1997) BRCA 1 and 2--A Genetic Link to Familial Breast and Ovarian Cancer. *Medscape women's health*, 2, 7.

34 Seftel, H.C., Baker, S.G., Jenkins, T. and Mendelsohn, D. (1989) Prevalence of familial hypercholesterolemia in Johannesburg Jews. *Am J Med Genet*, 34, 545-547.

35 Cai, X., Chiu, Y.H. and Chen, Z.J. (2014) The cGAS-cGAMP-STING pathway of cytosolic DNA sensing and signaling. *Molecular cell*, 54, 289-296.

bioRxiv preprint doi: https://doi.org/10.1101/402495; this version posted August 28, 2018. The copyright holder for this preprint (which was not certified by peer review) is the author/funder, who has granted bioRxiv a license to display the preprint in perpetuity. It is made available under aCC-BY 4.0 International license.

36 West, A.P., Khoury-Hanold, W., Staron, M., Tal, M.C., Pineda, C.M., Lang, S.M., Bestwick, M., Duguay, B.A., Raimundo, N., MacDuff, D.A. *et al.* (2015) Mitochondrial DNA stress primes the antiviral innate immune response. *Nature*, 520, 553-557.
37 Fang, C., Wei, X. and Wei, Y. (2016) Mitochondrial DNA in the regulation of innate immune responses. *Protein & cell*, 7, 11-16.
38 Crow, Y.J., Leitch, A., Hayward, B.E., Garner, A., Parmar, R., Griffith, E., Ali, M., Semple, C., Aicardi, J., Babul-Hirji, R. *et al.* (2006) Mutations in genes encoding ribonuclease H2 subunits cause Aicardi-Goutieres syndrome and mimic congenital viral brain infection. *Nat Genet*, 38, 910-916.
39 Dib, B., Lin, H., Maidana, D.E., Tian, B., Miller, J.B., Bouzika, P., Miller, J.W. and Vavvas, D.G. (2015) Mitochondrial DNA has a pro-inflammatory role in AMD. *Biochim Biophys Acta*, 1853, 2897-2906.
40 Hendrickson, S.L., Lautenberger, J.A., Chinn, L.W., Malasky, M., Sezgin, E., Kingsley, L.A., Goedert, J.J., Kirk, G.D., Gomperts, E.D., Buchbinder, S.P. *et al.* (2010) Genetic variants in nuclear-encoded mitochondrial genes influence AIDS progression. *PLoS ONE*, 5, e12862.
41 Nagase, T., Ishikawa, K., Suyama, M., Kikuno, R., Miyajima, N., Tanaka, A., Kotani, H., Nomura, N. and Ohara, O. (1998) Prediction of the coding sequences of unidentified human genes. XI. The complete sequences of 100 new cDNA clones from brain which code for large proteins in vitro. *DNA research : an international journal for rapid publication of reports on genes and genomes*, 5, 277-286.
42 Beier, U.H., Angelin, A., Akimova, T., Wang, L., Liu, Y., Xiao, H., Koike, M.A., Hancock, S.A., Bhatti, T.R., Han, R. *et al.* (2015) Essential role of mitochondrial energy metabolism in Foxp3(+) T-regulatory cell function and allograft survival. *Faseb J*, 29, 2315-2326.
43 Green, T.J., Benkendorff, K., Robinson, N., Raftos, D. and Speck, P. (2014) Anti-viral gene induction is absent upon secondary challenge with double-stranded RNA in the Pacific oyster, Crassostrea gigas. *Fish & shellfish immunology*, 39, 492-497.
44 Bellizzi, D., D'Aquila, P., Giordano, M., Montesanto, A. and Passarino, G. (2012) Global DNA methylation levels are modulated by mitochondrial DNA variants. *Epigenomics*, 4, 17-27.
45 Atilano, S.R., Malik, D., Chwa, M., Caceres-Del-Carpio, J., Nesburn, A.B., Boyer, D.S., Kuppermann, B.D., Jazwinski, S.M., Miceli, M.V., Wallace, D.C. *et al.* (2015) Mitochondrial DNA variants can mediate methylation status of inflammation, angiogenesis and signaling genes. *Hum Mol Genet*, 24, 4491-4503.
46 Smiraglia, D.J., Kulawiec, M., Bistulfi, G.L., Gupta, S.G. and Singh, K.K. (2008) A novel role for mitochondria in regulating epigenetic modification in the nucleus. *Cancer biology & therapy*, 7, 1182-1190.
47 Naviaux, R.K. (2008) Mitochondrial control of epigenetics. *Cancer biology & therapy*, 7, 1191-1193.
48 Wallace, D.C. and Fan, W. (2010) Energetics, epigenetics, mitochondrial genetics. *Mitochondrion*, 10, 12-31.
49 Morgan, A.E., Davies, T.J. and Mc Auley, M.T. (2018) The role of DNA methylation in ageing and cancer. *The Proceedings of the Nutrition Society*, in press., 1-11.

bioRxiv preprint doi: https://doi.org/10.1101/402495; this version posted August 28, 2018. The copyright holder for this preprint (which was not certified by peer review) is the author/funder, who has granted bioRxiv a license to display the preprint in perpetuity. It is made available under aCC-BY 4.0 International license.

Table 1

Cybrid	Gender	Age	Haplogroup
11-10	M	30	H4a1a
11-35	F	30	H1
13-52	F	58	H1
13-65	F	52	H41a1a
13-57	F	45	K1a1
13-65	F	38	K1a1b1a
13-75	F	56	K1c2
13-77	F	57	K1a1b1a
13-80	F	46	K1a1b2a1a

bioRxiv preprint doi: https://doi.org/10.1101/402495; this version posted August 28, 2018. The copyright holder for this preprint (which was not certified by peer review) is the author/funder, who has granted bioRxiv a license to display the preprint in perpetuity. It is made available under aCC-BY 4.0 International license.

Table 2

Target	Drugs	Cancer
EGFR	**Cetuximab (Erbitux), Eriotinib (Tarceva), Gefitinib (Iressa), Lapatinib (Tykerb)**	**non-small cell lung cancer, pancreatic cancer, breast cancer, colon cancer**
ALK	**Crizotinib (Xalkori), Certinib (Zykadia), Alectinib (Alecensa)**	**non-small cell lung cancers**
PD1	**Pembrolizumab (Keytruda), Nivolumab (Opdivo)**	**melanomas, non-small cell lung cancer, renal, bladder, head and neck cancers, Hodgkin lymphoma**

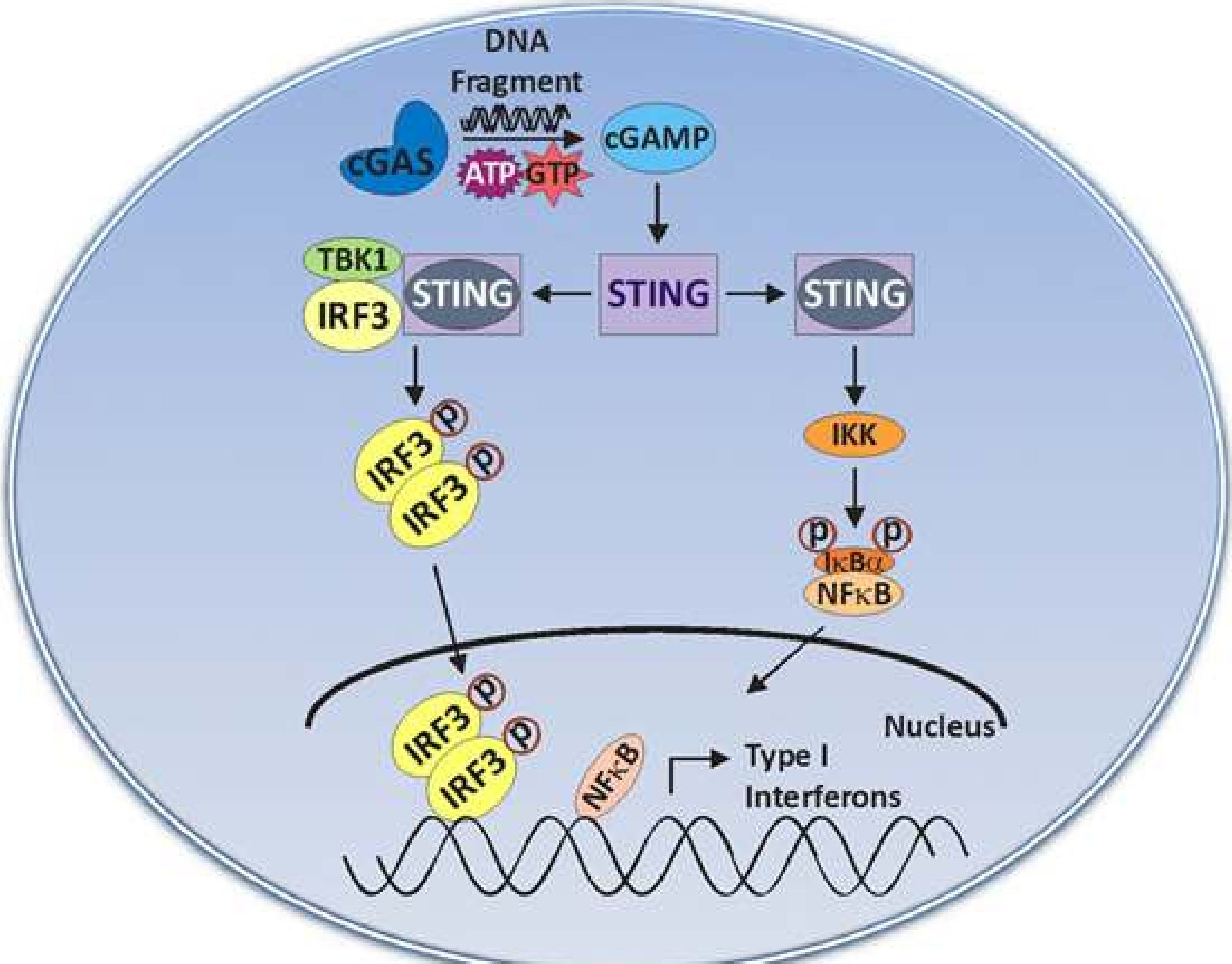
DNA
Fragment
cGAS
ATP
GTP
cGAMP
TBK1
IRF3
STING
STING
STING
IRF3
P
IRF3
P
IKK
P
P
IκBα
NFκB
IRF3
P
IRF3
P
Nucleus
NFκB
Type I
Interferons

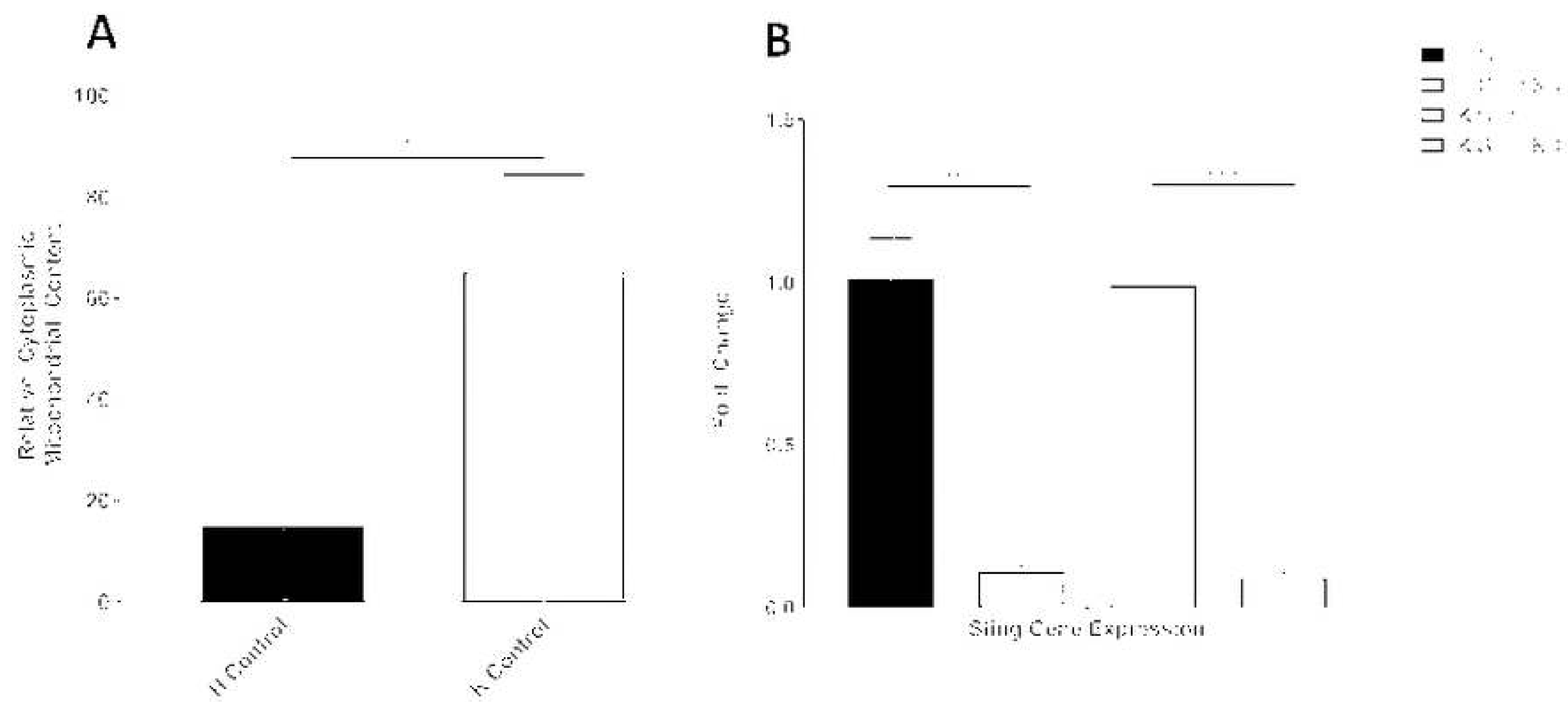
A
B

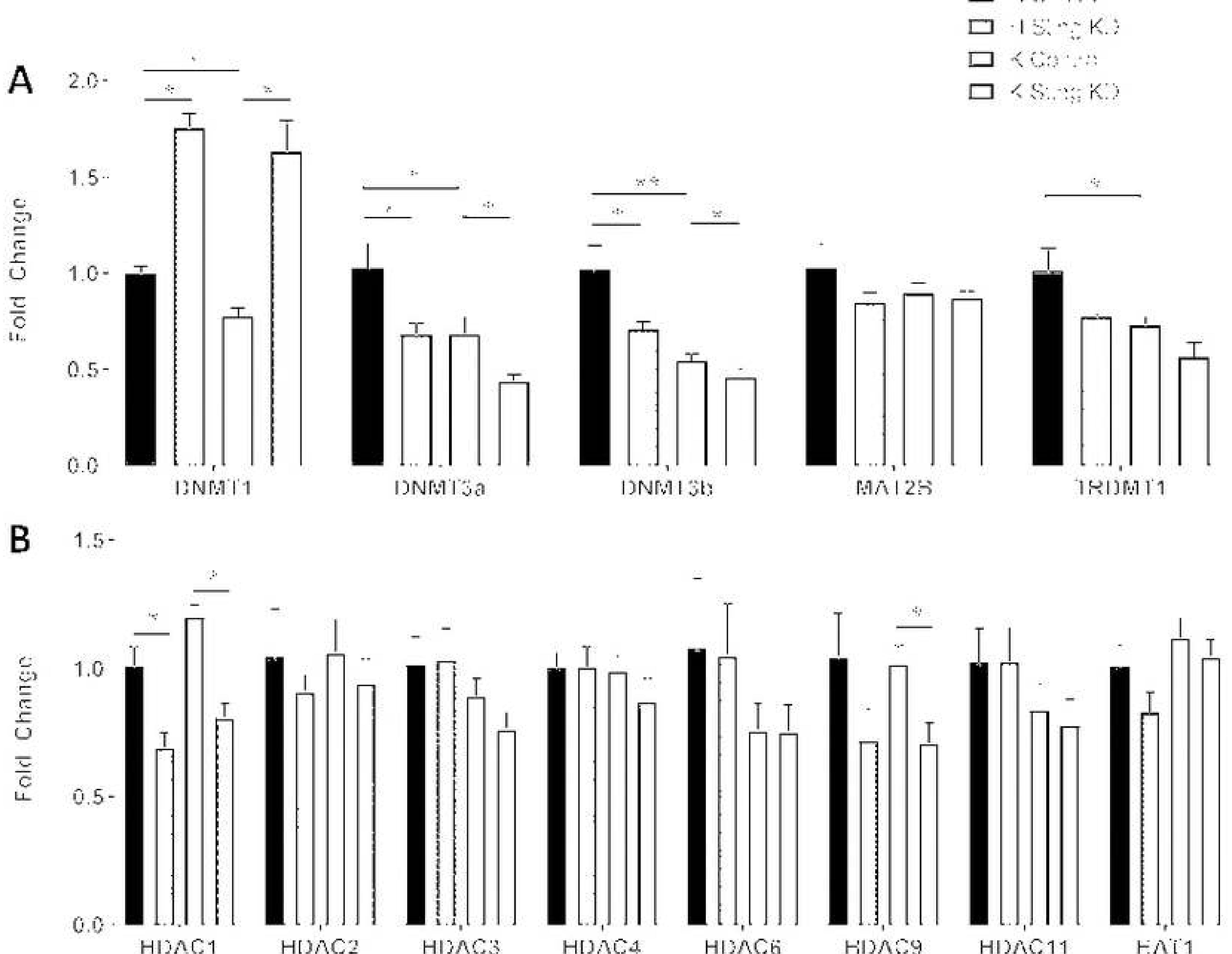
A
B
Fold Change
Fold Change
2.0
1.5
1.0
0.5
0.0
DNMT3a
HDAC1
HDAC2
HDAC3
HDAC4
HDAC6
HDAC9
HDAC11

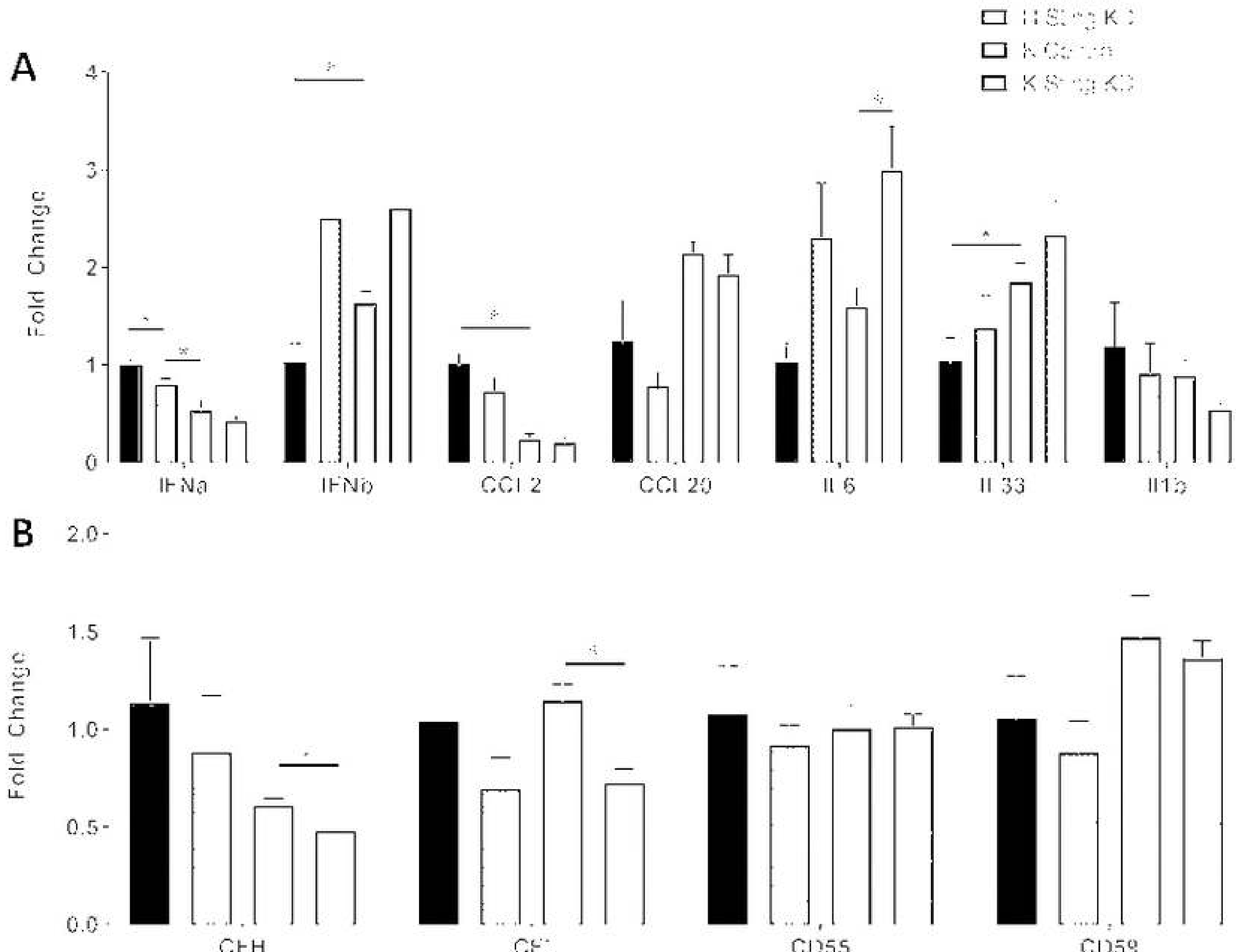
A
B
Fold Change
IFNa
IFNb
CCL2
CCL20
IL6
IL33
IL1b
CFH
CFI
CD55
CD59
0
1
2
3
4
0.0
0.5
1.0
1.5
2.0

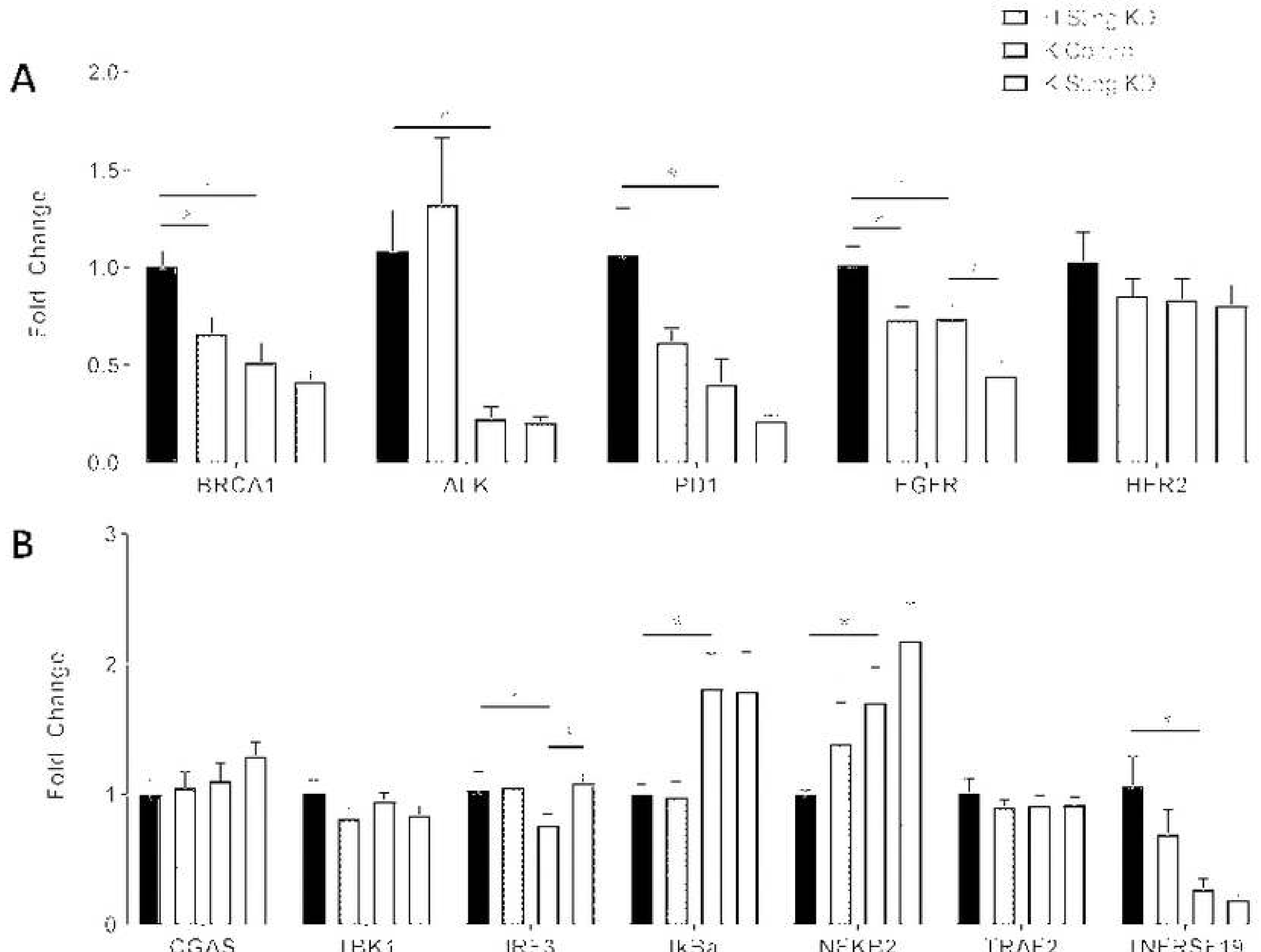
A
B
Fold Change
2.0
1.5
1.0
0.5
0.0
BRCA1
ALK
PD1
EGFR
HER2
Fold Change
3
2
1
0
CGAS
TBK1
IRF3
IkBa
NFKB2
TRAF2
TNFRSF19

A

H Cybrid K Cybrid

IRF3 ~47kD

b-actin ~42kD

Relative Protein Level of IRF3

8 6 4 2 0

**

H Untreated K Untreated

B

H Cybrid K Cybrid

p-IRF3 ~47kD

b-actin ~42kD

Relative Protein Level of p-IRF3

1.5 1.0 0.5 0.0

*

H Untreated K Untreated

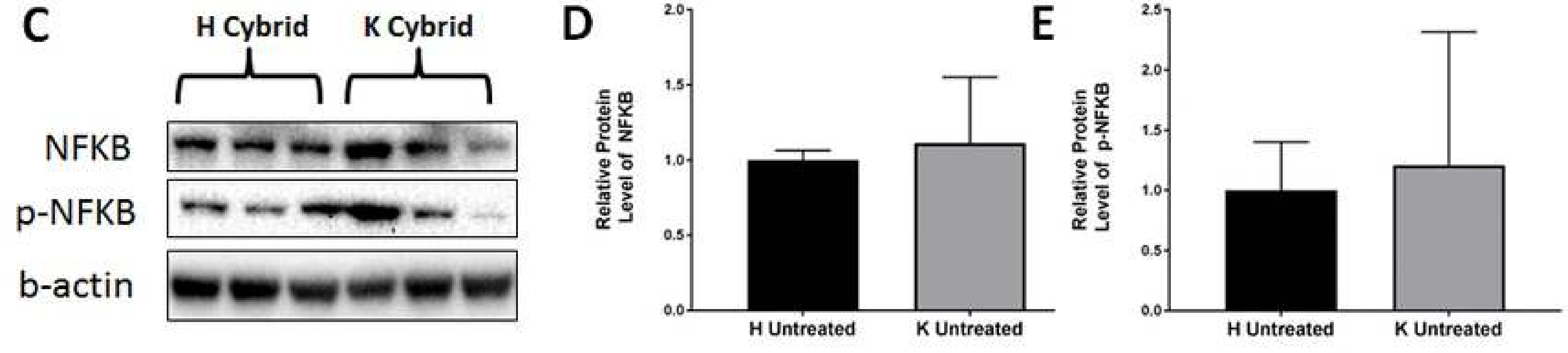

A

	Influenced by Haplogroup	Influenced by STING	Influenced differentially by both Haplogroup and STING
DNA Methylation			
DNMT1	Yes	Yes	No
DNMT3a	Yes	Yes	No
DNMT3b	Yes	Yes	**Yes****
TRDMT1	Yes	No	No
Histone Deacetylation			
HDAC1	No	Yes	No
HDAC9	No	Yes	**Yes****
Inflammation			
IFNa	Yes	Yes	**Yes****
IFNb	Yes	No	No
CCL2	Yes	No	No
IL33	Yes	No	No
CFI	No	Yes	**Yes****
CFH	No	Yes	**Yes****
IL6	No	Yes	**Yes****
Cancer			
BRCA	Yes	Yes	**Yes****
EGFR	Yes	Yes	No
ALK	Yes	No	No
PD1	Yes	No	No
ERBB	No	No	No
STING Pathway			
IkBa	Yes	No	No
NFKB2	Yes	No	No
TNFRSF19	Yes	No	No
IRF3	Yes	Yes	**Yes****
CGAS	No	No	No
TBK1	No	No	No